Validation of a 37-year Metocean Hindcast along the U.S. Atlantic Coast

Chi Qiao
Graduate Student, Dept. of Civil & Environmental Engineering, Northeastern University, Boston, U.S.A.

Andrew T. Myers
Associate Professor, Dept. of Civil & Environmental Engineering, Northeastern University, Boston, U.S.A.

Sanjay R. Arwade
Professor, Dept. of Civil & Environmental Engineering, University of Massachusetts, Amherst, U.S.A.

ABSTRACT: A numerical model is implemented using Mike 21 to estimate metocean conditions to evaluate hurricane risk for the 22 proposed wind energy areas along the U.S. Atlantic coast. A metocean hindcast study is conducted using this model for the period between 1979 and 2015 when atmospheric conditions are available as part of the Climate Forecast System Reanalysis (CFSR) study. These atmospheric conditions are used as input to the Mike 21 model, and the model results are compared with measurements of wind speed and significant wave height from five offshore buoys and of water level from three onshore stations. The predictions match the measurements reasonably well. The model is then applied to generate maps of wind speeds and wave heights with a 50-year return period, based on annual maxima of wind and wave.

1. INTRODUCTION

The offshore wind industry is growing in the United States. In pursuit of national goals of 22 GW of offshore wind capacity by 2030 and 86 GW by 2050 (Smith et al. 2015), a total of 27 wind energy areas (WEAs) have been designated by the U.S. government (BOEM 2017), and 22 of these are located along the Atlantic coast, where offshore wind turbines are exposed to hurricane risk. The metocean response under various atmospheric conditions can be estimated using a numerical model that considers the complex effects of bathymetry, coastline, and interactions between various hazards. A hindcast study on the metocean conditions using a numerical model provides a useful estimation of metocean conditions that are continuous in both time and space, but this model must first be validated with measurements, which are characteristically sparse in space and not continuous in time.

For this purpose, a regional model that covers the entire U.S. Atlantic coast is implemented here using the commercial software Mike 21 (referred to herein as the Mike 21 model). In this implementation, the hydrodynamic and spectral wave modules are coupled to simulate the metocean conditions. This model is intended to assess the hurricane risk imposed on offshore wind turbines and to provide site-specific metocean conditions for design purposes. Due to the low frequency and short historical record of hurricanes (~150 years for trajectories; ~20 years for detailed hindcast), synthetic catalogs of hurricanes are usually used to represent potential hurricane events for a much longer period, so that hurricane risk can be reliably evaluated. The Mike 21 model provides some unique features compared to other numerical models in the literature (Eungsoo Kim 2013; Westerink et al. 2008): first, it includes a coupled simulation of hydrodynamics and waves to provide more

consistent predictions of multiple metocean hazards and, second, it has a mesh size that is suitable for evaluating conditions at the 22 proposed WEAs using a 100,000-year synthetic hurricane catalog (Liu 2014).

In this paper, a 37-year (1979-2015) hindcast study is conducted using the Mike 21 model and atmospheric conditions from the Climate Forecast System Reanalysis (CFSR) study (Saha et al. 2011). The Mike 21 model is first validated with measurements of significant wave heights and water levels and then used to generate maps of wind and wave with a 50-year return period.

The details of the Mike 21 model and an introduction to the CFSR study are introduced in Section 2. Metocean measurements that are used for validation are introduced in Section 3. The results of the validation are discussed in Section 4, and the wind and wave maps with 50-year mean return periods are presented in Section 5. Conclusions are provided in Section 6.

2. METOCEAN MODELING

Details of the Mike 21 model are introduced in this section, including definition of the model domain and mesh and important physical phenomena considered in the simulation. Details of the atmospheric conditions estimated as part of the CFSR study are also introduced.

2.1. Mike 21

An unstructured mesh covering the entire U.S. Atlantic coast is used for the metocean hindcast. The mesh domain is extended southward to the islands in Caribbean Sea to form a closed boundary. The spatial resolution of the mesh varies approximately linearly with the water depth, varying between 20 km for deep water areas and 5 km for shallow water areas, and totaling ~66,000 triangular elements (Figure 1). The bathymetry is linearly interpolated from the Global Relief Model (Amante and Eakins 2009) for most of the model domain and the Coastal Relief Model (NOAA 2008) for some portions of the domain with shallow water.

Mike 21 includes various modules for simulations of different physical phenomena. In this study, the hydrodynamic (HD) and spectral wave (SW) modules are coupled. The HD module simulates ocean hydrodynamics using the depth-integrated, incompressible, Reynolds-averaged Navier-Stokes equations (DHI 2014), while the SW module simulates the growth, propagation and decay of wind-generated waves and swell based on a wave action conservation equation (DHI 2014). The HD and SW modules are coupled such that the modeling of wave propagation in the SW module includes the effects of changes to the still water depth and current. Both modules require the wind field at 10 m height as input, and the HD module also requires atmospheric pressure field at mean sea level.

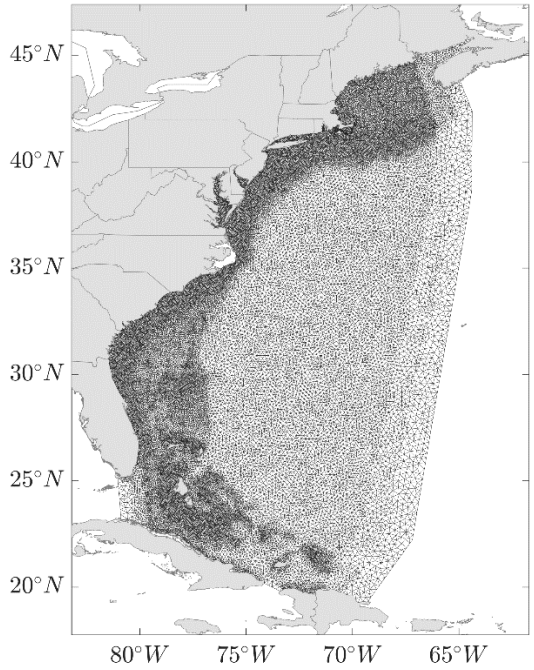

Figure 1: Unstructured mesh of the Mike 21 model domain.

In the HD module, the sea bed resistance is modeled with a constant Manning number of 32 $m^{1/3}/s$ for the entire domain. Wind friction is modeled using the drag coefficient proposed by Wu (Wu 1994). Tide levels are specified along the open boundaries of the model using the DHI Global Tide Model (DHI 2014). In the SW module, frequency is discretized into 40 bins logarithmically between 0.03 Hz and 1.42 Hz, and

wave direction is discretized into 36 bins with constant intervals of 10°. Dissipation of energy due to depth-induced wave breaking is modeled following the formulation by Battjes and Janssen (Battjes and Janssen 1978). Bottom friction is modeled using a constant Nikuradse roughness (Weber 1991) of 0.04 m. The equation proposed by Bidlot et al. (Bidlot et al. 2007) is used to describe dissipation of energy due to white capping. A lateral boundary is applied in the SW module, meaning that the effect of waves propagating from outside the boundary is neglected.

2.2. CFSR wind and pressure fields

The CFSR wind and pressure fields are generated from a reanalysis using the Climate Forecast System (CFS). This reanalysis assimilates data from satellite radiances and all available conventional observations (e.g., buoy measurements and ship observations) at 6-hour intervals and uses a coupled atmosphere-ocean-land model for making hourly forecasts. The reanalysis data used in this study (Saha et al. 2010; Saha et al. 2011) is obtained from two separate versions of the CFS. Both versions provide information at 1-hour intervals and the older one, which covers the time period 1979-2011, has a slightly coarser spatial resolution of 0.31° than the newer one, which covers the time period 2011-2016 with a spatial resolution of 0.21°. The information from both versions is interpolated here to the resolution of 0.054° using cubic interpolation.

Note that the wind reanalysis data is a mean wind speed, provided at the height of 10 m. As such, it is directly used for Mike 21 input without conversion for averaging time (Harper et al. 2008) or height.

3. VALIDATION DATASETS

Predictions of significant wave height (H_s) and water level (η) from Mike 21 and wind speed (V) from CFSR are validated against measurements in this paper. Measurements during 1979-2015 from the NDBC (National Data Buoy Center) and NOS (National Ocean Service) network, and the CO-OPS (Center for Operational Oceanographic Products and Services) are considered in this study. Five buoys which record wind speeds and wave heights, and three onshore stations, which record water levels, are selected for validation of the Mike 21 model (Figure 2). They are selected to cover most of the model domain and hindcast period (Figure 3).

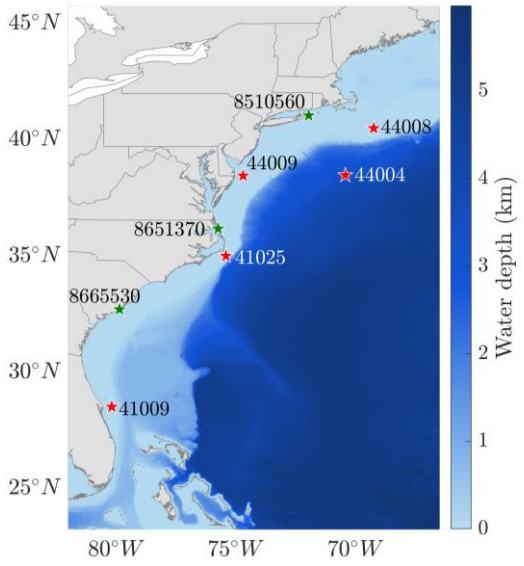

Figure 2: Location of the five buoys (red stars) and three water level stations (green stars) where measurements are used for validation. The color indicates water depth.

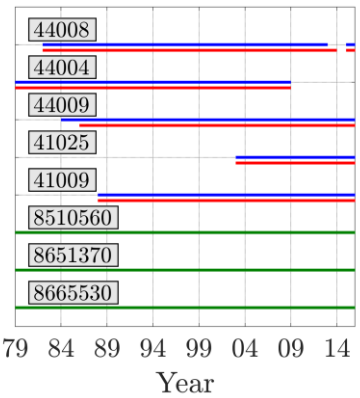

Figure 3: Period of measurement for the five buoys and three water level stations in Figure 2. Blue, red, and green lines represent wind speed, wave height, and water level, respectively.

Metocean measurements (i.e., $V, H_s, \& \eta$) are recorded at various intervals, ranging from five minutes to one hour, and measurements of wind speed are averaged over an eight-minute period and recorded at 5 m. When comparing with model predictions, all measurements are converted to 1-hour intervals, and wind speeds are converted to values at 10 m elevation, using the power law profile with coefficient of 0.14 (IEC 2009).

4. RESULT AND DISCUSSION

Hindcast results of wave, water level, and wind are validated against measurements in this section. Detailed validation results are presented for five buoys recording wind speeds and wave heights and for three onshore stations recording water levels.

Various approaches are used to compare the hindcast results with measurements. Bias of the monthly mean is first analyzed to evaluate the overall behavior of the results. Distributions of the hourly data and the annual maxima are then analyzed using a quantile-quantile (Q-Q) plot where the quantiles of one dataset are compared with the quantiles of another dataset. And lastly the correlation coefficient and two statistical error terms are evaluated in a Taylor diagram (Taylor 2001) for hourly data during each year. A Taylor diagram plots the correlation coefficient in terms of the azimuthal angle, the standard deviation in terms of the distance to the origin, and the centered root-mean-square error (CRMSE) in terms of the distance to the reference point. Values in the Q-Q plot are normalized using the maximum measurement, so that wind and wave at the same location can be shown on the same scale. For the same purpose, the data in the Taylor diagram is also normalized, where normalized CRMSE is defined as,

$$CRMSE = \frac{\sqrt{\overline{\left((x_p - \bar{x}_p) - (x_m - \bar{x}_m)\right)^2}}}{\sqrt{\overline{(x_m - \bar{x}_m)^2}}}$$

and normalized standard deviation σ_n is defined as,

$$\sigma_n = \frac{\sqrt{\overline{(x_p - \bar{x}_p)^2}}}{\sqrt{\overline{(x_m - \bar{x}_m)^2}}}$$

where x_p is the prediction from the hindcast result and x_m is the measurement.

4.1. CFSR wind

The bias of the monthly mean is shown in Figure 4(a) for the five selected buoys. Two outliers are observed for Buoy 44008 between Nov. 1984 and Jan. 1985, and, for Buoy 44009, during Feb. 2013, and the corresponding measurements are considered as errors and ignored in the following validation. For the latter outlier, the bias in CFSR wind is most likely due to malfunction of the anemometer, as the outlier is included in a period of several days when measurements are approximately zero.

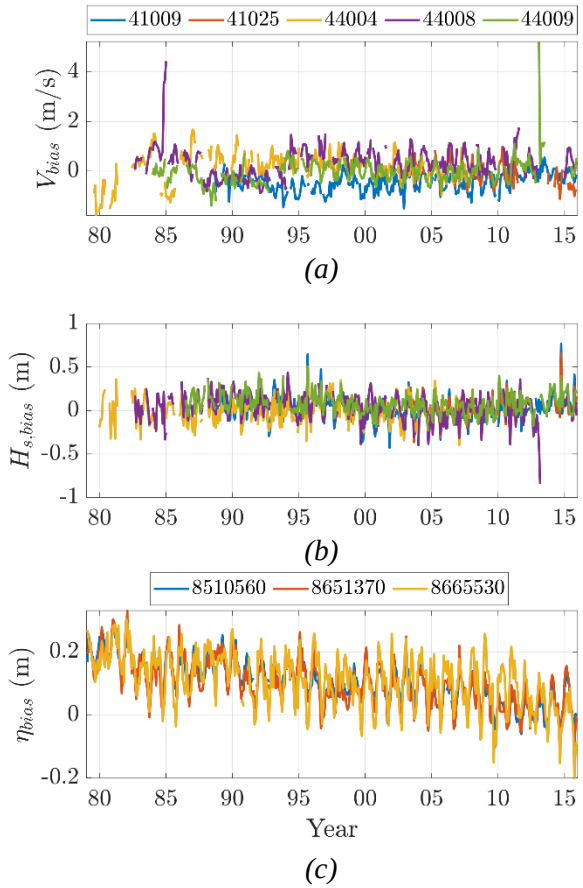

Figure 4: Monthly mean bias of a) V, b) H_s, and c) η.

The Q-Q plot of the hourly wind data (first column of Figure 5) shows a reasonable match between CFSR wind and measurement, indicating that they follow the same distribution. The annual maxima data also shows a reasonable match (second column of Figure 5), except for Buoy 44009, where CFSR wind tends to overestimate the high wind speeds. The evaluation for the annual maximum winds is important when the dataset is extrapolated for the extreme values. The Taylor diagrams (third column of Figure 5) indicate consistent performance year to year, and the data clusters at the correlation coefficient of 0.90 and normalized standard deviation of 1.0 for all selected buoys.

4.2. Wave hindcast

The bias of the monthly mean of wave height is small for all selected buoys except for Buoy 44008 during Mar. 2013, when one significant underestimation is observed (Figure 4(b)). The time history comparison between the hindcast and measurement for this underestimation shows that several peaks in the measurement, which are probably induced by intense storms, are not simulated in the hindcast. Unfortunately, no wind speed measurement is available during this period, and thus it is difficult to know whether the underestimation is a result of error in the CFSR wind input.

The Q-Q plot of the hourly data (first column of Figure 5) shows a reasonable match of the distribution between hindcast and measurement except for Buoys 44008 & 44009 where hindcast tends to underestimate wave heights. Such underestimation also affects the distribution of the annual maxima (second column of Figure 5). A significant underestimation is observed for the hourly data of Buoy 41025 in Figure 5, which corresponds to one measurement during hurricane Isabel in 2003. This is most likely due to the error in the measurement, as, during this hurricane, the measurement increased from 8.2 m to 13.6 m in one hour, after which the measurements stopped. In the Taylor diagrams (third column of Figure 5), the wave hindcast results show more scattering than the wind inputs, and the data clusters at the correlation coefficient of 0.90 and normalized standard deviation less than 1.0.

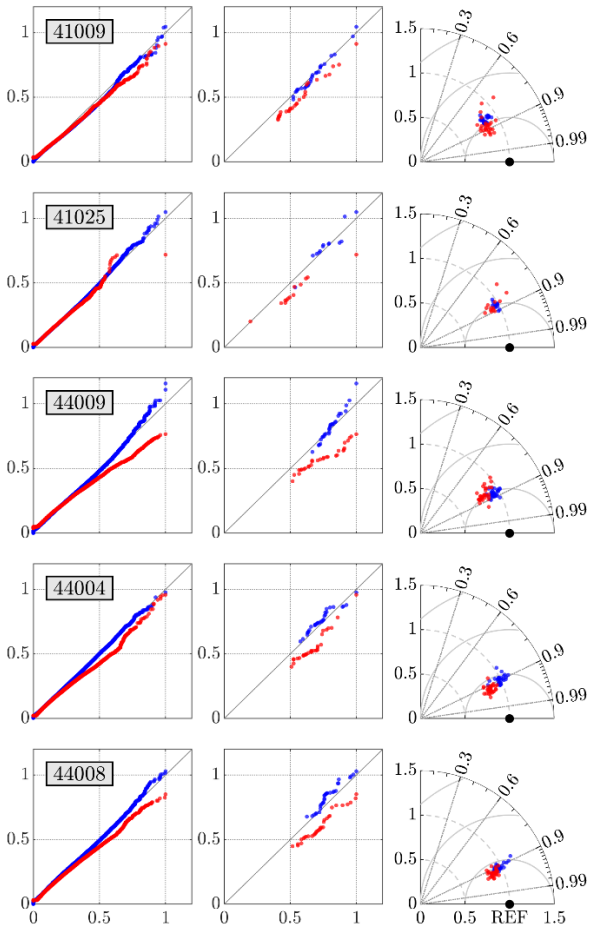

Figure 5: Comparison for V (in blue) and H_s (in red). The first column is the Q-Q plot of the hourly data with measurements on the horizontal axis and hindcast results on the vertical axis, and with data normalized by their maxima. The second column is similar to the first column but instead shows annual maxima data. The third column is the Taylor diagram showing normalized statistics of the annual data.

4.3. Water level hindcast

A linear trend is observed in the bias of the monthly mean plot (Figure 4(c)), which is because the change in the mean sea level is not considered in the simulation, and thus hindcast data is corrected for the bias during the following validation.

Both the hourly data and annual maxima show a reasonable match between prediction and

measurement (Figure 6), except for one hour of significant underestimation at Station 8665530, which occurs during hurricane Hugo in 1989. The annual maxima data in the Taylor diagram shows more consistent performance than wind and wave, with correlation coefficient around 0.90 and normalized standard deviation approximately 1.0. This is not surprising, as water level is usually dominated by tides, which is relatively easy to predict, and only influenced by storm surge occasionally.

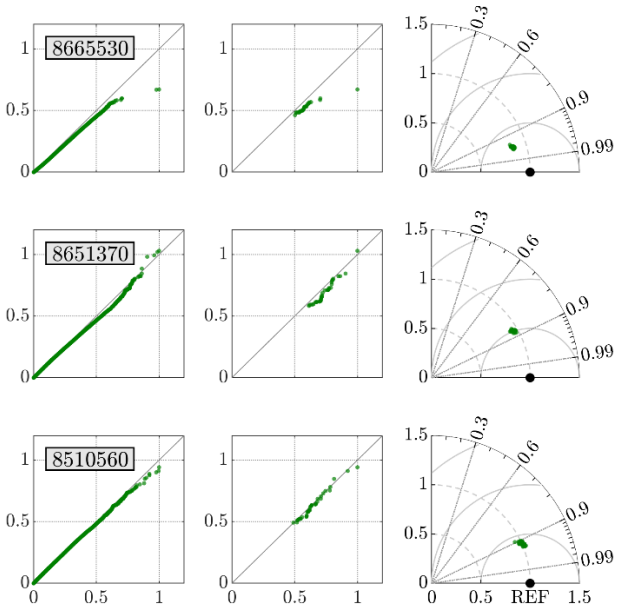

Figure 6: Similar to Figure 5, but for η.

5. 50-YEAR NON-HURRICANE WIND & WAVE MAP

Validation results in Section 4 show an overall good prediction performance of the Mike 21 model. The resulting 37-yr metocean hindcast from the Mike 21 model can be used to determine the environmental conditions along the U.S. Atlantic coast for the design of offshore structures. The 50-year values of wind and wave are presented here for an area that includes all locations at least 100 km from the coastline and includes all the WEAs proposed along the U.S. Atlantic coast.

This area is prone to hurricane hazard, and the wind induced by hurricane follows a different mechanism than the non-hurricane winds. As such, the long-term hurricane conditions are usually predicted from a much longer period (Vickery et al. 2009) and they are not considered here. Metocean conditions induced by hurricanes are discarded from the hourly hindcast results, where hurricane events are defined here as the hours with a distance to the hurricane eye less than 250 km, based on hurricane trajectories obtained from the HurDat2 database (Landsea et al. 2015). The 50-year values are extrapolated from the distribution of 37 annual maxima with hurricane excluded using the Gumbel distribution. The parameters of the Gumbel distribution are obtained using the least squares approximation through the Gumbel chart, which plots the data in ascending order on the horizontal axis and the corresponding reduced variate on the vertical axis, where the reduced variate is defined as $-\ln(-\ln(F_x))$ with, in this case, F_x determined by the empirical cumulative density function. A Gumbel distribution fits the data well for both wind and wave (see insets of Figure 7 & 8 at the location of Buoy 44009 as an example). The 50-year values are then determined from F_x of annual maxima at the value of $1 - 1/50 = 0.98$, which corresponds to the reduced variate on the Gumbel chart of 3.90.

The 50-year wind map excluding hurricanes (Figure 7) shows a higher wind speed in the north, where winter storms are more frequent. Two hot spots are observed in the map near Massachusetts and South Carolina. Note that the hot spot near South Carolina might still be affected by hurricanes, as the 250 km threshold might be too low for intense hurricanes and hurricanes with large radius to maximum wind.

The 50-year wave map excluding hurricanes (Figure 8) shows a similar spatial trend and similar locations of hot spots as the map of wind. Note that propagation of waves is a complicate nonlinear process, affected by wind speed, water depth, and fetch length, etc. As such, the high wind speeds and relatively deep water near Massachusetts and South Carolina result in the high values of significant wave height.

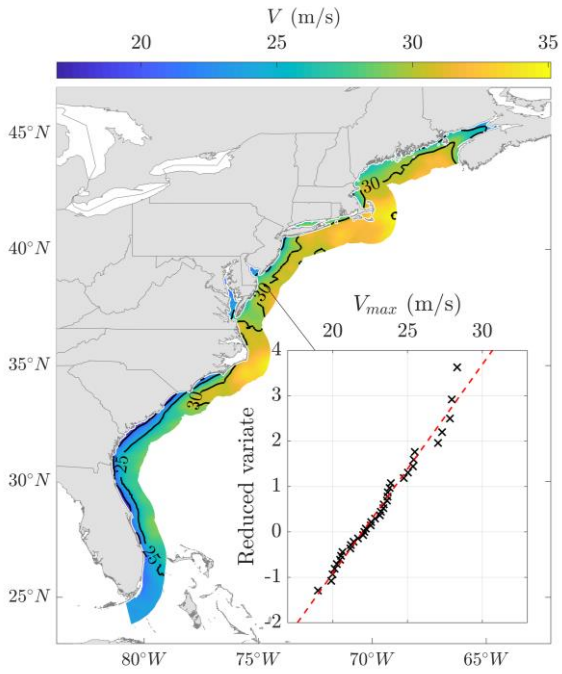

Figure 7: 50-year wind map at 10 m for U.S. Atlantic offshore area, excluding hurricanes. The inset figure shows the Gumbel fitting for the location of Buoy 44009 for annual maxima on the horizontal axis and reduced variate on the vertical axis.

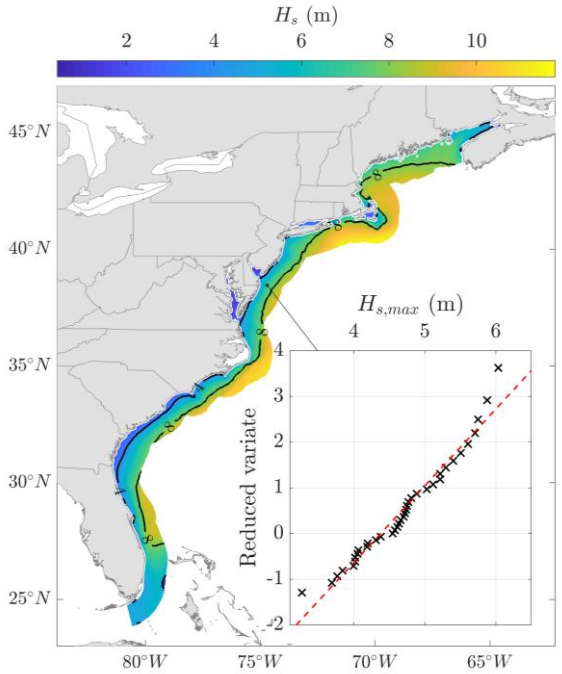

Figure 8: Similar to Figure ,7 but for 50-year significant wave height, excluding hurricanes.

6. CONCLUSIONS

A 37-year hindcast of metocean conditions covering the period from 1979 to 2015 is constructed using a numerical model implemented in the commercial program Mike 21. The atmospheric inputs which drive the Mike 21 model are taken from a reanalysis study and the hindcast results are validated using five offshore buoys for wind speeds and significant wave heights and three onshore stations for water levels.

The hindcast results are compared with the measurements in terms of the monthly mean bias, the distribution of the hourly and annual maxima data, and a Taylor diagram. A detailed validation shows that the measurements need to be carefully examined for any problematic recordings, especially during intense storms. No significant bias is observed for wave hindcast, while the monthly mean bias of water level indicates the need for a linear correction of the water level to account for the change in mean sea level. The distributions of hourly and annual maxima data show a reasonable match for water level, though some underestimation is observed for two buoys. Taylor diagrams show a similar performance for both wave and water level, with a correlation coefficient of ~0.90 and a normalized standard deviation of ~1.0, while the annual maxima data from the wave hindcast exhibits more scattering.

The 50-year values of wind and wave, excluding hurricanes, are plotted for the U.S. Atlantic coast. The wind speeds and wave heights are extrapolated to a return period of 50 years using annual maxima data. For both wind and wave, the map shows higher value in the north compared to south, with two hot spots near Massachusetts and South Carolina.

7. REFERENCES

BOEM. (2017). "Wind Planning Areas (Shapefile)."

Amante, C., and Eakins, B. W. (2009). "ETOPO1 1 Arc-Minute Global Relief Model: Procedures, Data Sources and Analysis." *NOAA Technical Memorandum NESDIS NGDC-24. National Geophysical Data Center, NOAA.*

Battjes, J., and Janssen, J. (1978). "Energy loss and set-up due to breaking of random waves." *Coastal Engineering Proceedings*, 1(16).

Bidlot, J., et al. (2007). "A revised formulation of ocean wave dissipation and its model impact."

DHI (2014). *MIKE21-FM HD Scientific Documentary*, DHI Water and Environment, Denmark.

DHI (2014). *MIKE21 SW Scientific Documentary*, DHI Water and Environment, Denmark.

DHI (2014). *MIKE 21 Toolbox -Global Tide Model - Tide prediction*, DHI Water and Environment, Denmark.

Eungsoo Kim, L. M. (2013). "Coupled Atmosphere-Wave-Ocean Modeling to Characterize Hurricane Load Cases for Offshore Wind Turbines." *51st AIAA Aerospace Sciences Meeting including the New Horizons Forum and Aerospace Exposition*, American Institute of Aeronautics and Astronautics.

Harper, B., et al. (2008). "Guidelines for converting between different wind averaging periods in tropical cyclone conditions." *World Meteorological Organization*.

IEC (2009). "IEC 61400-3." *Design requirements for offshore wind turbines*.

Landsea, C., et al. (2015). "The revised Atlantic hurricane database (HURDAT2). United States National Oceanic and Atmospheric Administration's National Weather Service."

Liu, F. (2014). "Projections of Future US Design Wind Speeds Due to Climate Change for Estimating Hurricane Losses." Clemson University.

NOAA (2008). "U.S. Coastal Relief Model."

Saha, S., et al. (2010). "NCEP Climate Forecast System Reanalysis (CFSR) Selected Hourly Time-Series Products, January 1979 to December 2010." Research Data Archive at the National Center for Atmospheric Research, Computational and Information Systems Laboratory, Boulder, CO.

Saha, S., et al. (2011). "NCEP Climate Forecast System Version 2 (CFSv2) Selected Hourly Time-Series Products." Research Data Archive at the National Center for Atmospheric Research, Computational and Information Systems Laboratory, Boulder, CO.

Smith, A., et al. (2015). "2014-2015 Offshore wind technologies market report." National Renewable Energy Lab.(NREL), Golden, CO (United States).

Taylor, K. E. (2001). "Summarizing multiple aspects of model performance in a single diagram." *Journal of Geophysical Research: Atmospheres*, 106(D7), 7183-7192.

Vickery, P. J., et al. (2009). "U.S. Hurricane Wind Speed Risk and Uncertainty." *Journal of Structural Engineering*, 135(3), 301-320.

Weber, N. (1991). "Bottom friction for wind sea and swell in extreme depth-limited situations." *J Phys Oceanogr*, 21(1), 149-172.

Westerink, J. J., et al. (2008). "A basin- to channel-scale unstructured grid hurricane storm surge model applied to southern Louisiana." *Mon Weather Rev*, 136(3), 833-864.

Wu, J. (1994). "The sea surface is aerodynamically rough even under light winds." *Boundary-Layer Meteorology*, 69(1-2), 149-158.